Linear Free Energy Relationships in Hydrogen Evolution Catalysis by a Cobalt Tripeptide in Water

Journal:	*ACS Energy Letters*
Manuscript ID	nz-2021-00680n.R1
Manuscript Type:	Letter
Date Submitted by the Author:	n/a
Complete List of Authors:	Alvarez-Hernandez, Jose ; University of Rochester, Chemistry Han, Ji Won; University of Rochester, Department of Chemistry Sopchak, Andrew; University of Rochester, Department of Chemistry Guo, Yixing; University of Rochester, Department of Chemistry Bren, Kara; University of Rochester, Department of Chemistry

Linear Free Energy Relationships in Hydrogen Evolution Catalysis by a Cobalt Tripeptide in Water

Jose L. Alvarez-Hernandez, Ji Won Han, Andrew E. Sopchak, Yixing Guo, and Kara L. Bren*

Department of Chemistry, University of Rochester, Rochester, New York 14627-0216, United States.

*Corresponding author: Kara L. Bren, bren@chem.rochester.edu

Abstract

Water is the desired solvent for catalytic hydrogen production, but the presence of multiple proton donors in buffered water complicates analysis of reaction mechanisms. Here, we determine substrate-dependent rate constants for electrocatalytic hydrogen evolution by a cobalt tripeptide (CoGGH) in the presence of buffers of pK_a 6.9 to 10.4. Catalytic rate constants in the presence of buffer (k_{HA}) are two to four orders of magnitude higher than when water is the sole proton source, indicating that buffer acid outcompetes water as a proton donor. The rate of hydrogen evolution catalyzed by CoGGH is found to be dependent on the buffer-acid pK_a and independent of pH (from pH 8 to 10). A Brønsted-type linear free energy relationship between k_{HA} and buffer-acid pK_a is found, supporting a concerted proton-coupled electron transfer with a buffer conjugate acid proton donor as a common rate-determining step for the buffers used.

TOC Graphic

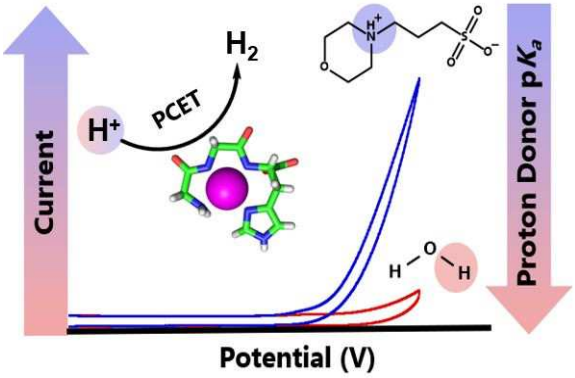

Hydrogen (H_2) can be used as both a carbon-free fuel and a chemical reductant, making the reduction of protons a reaction of high current interest.[1-3] Furthermore, insights from mechanistic studies of the catalytic hydrogen evolution reaction (HER) are helpful for building a better understanding of more complex reactions requiring proton transfers.[4-6] Among the many factors that impact HER catalysis, the effects of pH,[7-11] pK_a of exogenous acids and bases,[12-22] type of solvent,[23-25] protonatable sites on catalysts,[26-31] and the role of proton-coupled electron transfer (PCET)[4-6,32] have been highlighted. Furthermore, there has been a push to develop and study HER in water, rather than aprotic solvents or solvent mixtures.[10,33-38] Developing and understanding aqueous electrocatalysts is an important step toward their use in systems for water splitting, and utilizes a widely available, nontoxic solvent.

Buffers, though often overlooked, play important roles in aqueous electrocatalysis. Beyond maintaining the pH of the solution, buffers provide added acid/base species that may participate in proton transfer steps to or from the catalyst. Buffer species have been implicated in catalysis of CO_2 reduction,[39,40] proton reduction,[13,15,37] water oxidation,[41-44] and oxygen reduction,[22] with both buffer pK_a[13,15,22,40,41] and structure[15,39] having effects on catalysis. For example, for a cobalt-porphyrin mini-enzyme, we identified that the HER mechanism depends upon the buffer pK_a.[15] In another example, for a cobalt-porphyrin-peptide HER electrocatalyst, we found a switch in the rate-determining step of the catalytic cycle dependent upon the buffer-acid pK_a.[13] Despite the progress made, a deeper understanding of the roles played by both buffers and water in the mechanisms of catalytic reactions involving protons is very much needed.

Here, we report a linear free energy relationship for the rate of H_2 evolution from water with buffer-acid pK_a for HER catalyzed by CoGGH, a cobalt-tripeptide catalyst (Figure 1).[33,35] By studying the scan-rate-independent cyclic voltammetry (CV) responses of the catalyst in both buffered and unbuffered solutions, we deduced rate constants specific to catalysis in which water vs. a buffer conjugate acid is the proton donor (Table S1 lists the buffers used here along with abbreviations, structures, and pK_a values). This linear free energy relationship is interpreted in the context of the Brønsted law, providing insight into the identity of the proton donor and the concerted nature of PCET within the electrochemical HER mechanism for CoGGH.

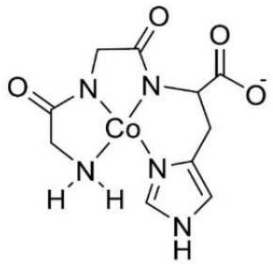

Figure 1. CoGGH (Cobalt-glycine-glycine-histidine). With cobalt as Co(III), CoGGH is a neutral complex referred to as **[1]**; the Co(II) form then corresponds to **[1]$^-$,** and so on.

Cyclic voltammetry of CoGGH in aqueous solution (pH 8.0) yields catalytic waves that develop at onset potentials of ~ –1.2 to –1.4 V vs. Ag/AgCl/KCl$_{(1M)}$ (all potentials here are reported

against this reference), previously shown to correspond to the reduction of protons to H_2.[33] The catalytic current is highly sensitive to both concentration and identity of the buffer present, although a weak response is also detected in the absence of buffer. Controlled potential electrolysis experiments show that faradaic efficiency for the HER does not vary significantly with buffer identity (Figure S1, Table S2). Figure 2a shows voltammograms of CoGGH collected at 0 – 70 mM MOPS buffer concentration and Figure 2b shows CVs in different buffers as well as pH-adjusted water containing only KCl (no buffer). The addition of buffer significantly enhances the catalytic current and shifts the onset potential anodically, suggesting that the buffer acid is outcompeting water as a proton donor. We have previously reported that buffer pK_a affects the kinetics of HER catalyzed by a cobalt-porphyrin-peptide catalyst in water,[13] as the strength of the acid determines the rate of proton transfer from the proton donor to the catalyst, a result also obtained in studies of organic acid proton donors to HER catalysts in aprotic media.[12,45]

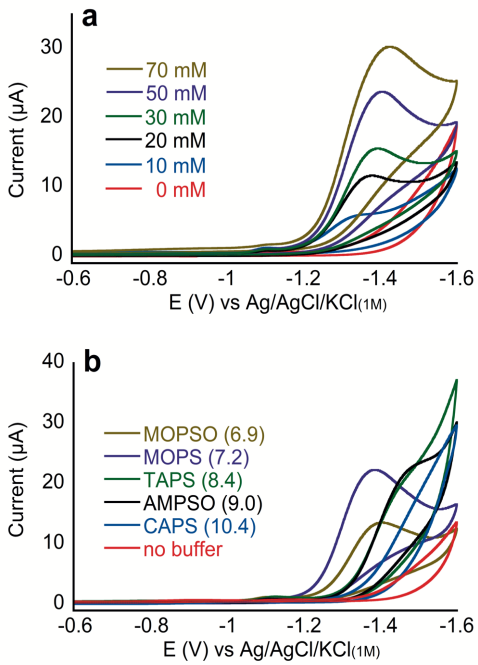

Figure 2. CVs of 50 μM CoGGH in **(a)** 0 to 70 mM MOPS **(b)** 50 mM of the indicated buffer as well as KCl electrolyte only. All data collected at 100 mV/s, 0.1 M KCl pH 8.0 scanning from 0 to −1.6 V in the cathodic (forward) scan and from −1.6 to 0 V in the anodic (reverse) scan. Buffer pK_a values shown in parenthesis

To determine rate constants for HER catalyzed by CoGGH, it is important to establish whether the catalytic activity arises from a homogeneous molecular species, an adsorbed molecular species,[46,47] or a catalytically active material that forms in situ.[48,49] To address this question, we performed rinse tests of the hanging mercury drop (HMDE) working electrode. Typically, post-CV rinse tests are performed on solid electrodes.[49] Here, we use a different procedure that we call a "dip-and-stir" (D-S) test, described in detail in the Experimental Section. The D-S test shows that catalysis is due to an adsorbed species and that adsorption takes place regardless of the applied potential and also at the open-circuit potential (Figure 3). The solution composition is also found

to have no effect on catalyst adsorption as shown in Figures S2-S8. A pre-catalytic wave is detected in the CV of CoGGH at ~ −1.10 V in the forward scan but is absent in the post-rinse voltammograms (Figure S3b), suggesting that the feature is associated with catalyst adsorption to the electrode. An oxidative peak at ~ −0.30 V is seen in the reverse scan, but only if the pre-catalytic wave is accessed in the forward scan (Figure S9). This oxidative feature significantly decreases over repetitive post-rinse CV scans (Figure S3d), consistent with desorption of the catalyst under those conditions. This adsorption-desorption process explains the differences seen in repetitive CV collected with and without CoGGH in solution as shown in Figure S3c. A concern with catalysts adsorbed to electrodes is the possibility of decomposition yielding metal nanoparticles that act as the active catalyst.[48,50,51] Here, the use of a mercury electrode obviates that concern as mercury amalgamates cobalt;[49,52] indeed, no activity from $CoCl_2$ is observed (Figure S10). We conclude that the adsorbed catalytically active species is molecular in nature.

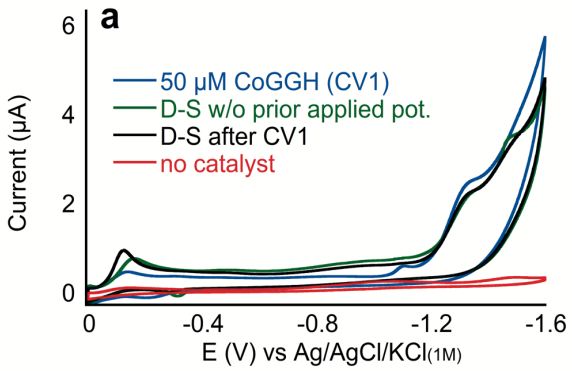

Figure 3. Results of D-S tests performed for 50 µM CoGGH, 0.1 M KCl pH 8.0 at 100 mV/s in 10 mM MOPS.

We will treat the system under consideration here as a catalytically active monolayer comprised of immobilized molecules of CoGGH, or another molecular species derived from it, and will determine rate constants for HER under this assumption. Equation 1 defines the maximum current for a monolayered electrocatalytic film operating under pure-kinetic conditions, i.e. no substrate consumption is taking place and a steady state is achieved between the active and resting states of the catalyst.[53] The derivation of equation 1 also assumes that both the electron transfer from the electrode to the adsorbed catalyst and the diffusion of the substrate from the solution to the electrode surface are fast relative to the catalytic rate, conditions both fulfilled at relatively high scan rates and buffer concentrations, or when the solvent (i.e. water) is the substrate.[53-55]

$$I_k = 2FAk\Gamma_{cat}[S] \quad (1)$$

Equation 1 applies to a two-electron process that is first order in both catalyst and substrate.[53,54] I_k corresponds to the catalytic current, F is the Faraday constant, A is the surface area of the working electrode, Γ_{cat} is the surface concentration of the catalyst, and [S] is the concentration of the substrate S.[53,54] At relatively low scan rates, the voltammograms are peaked and the peak current is linear with the square root of the scan rate, indicating that there is significant

substrate consumption and that the CV response is limited by diffusion of substrate to the electrode as seen in Figure 4a for voltammograms collected at 100 to 600 mV/s in MOPS-containing solutions (Figures S11-S15 show these data for all buffers).

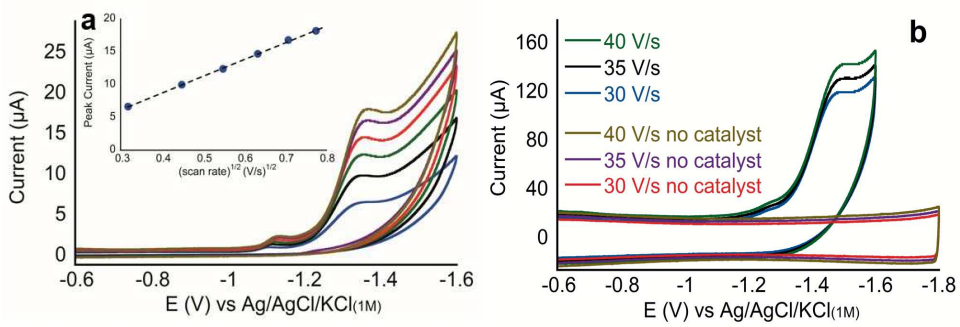

Figure 4. CVs of 50 μM CoGGH in 10 mM MOPS, pH 8.0, 0.1 M KCl. **(a)** Scan rates 100 to 600 mV/s in 100 mV/s increments. The inset shows the linear plot of peak current vs. the square root of the scan rate, consistent with the CV response determined by diffusion of buffer to the electrode. **(b)** Scan-rate independent CVs at 30 to 40 V/s, consistent with pure kinetic conditions governing the CV response.

At higher scan rates, 25 to 50 V/s, the CV response becomes scan-rate independent and the voltammogram peak is lost, consistent with no substrate depletion (pure kinetic conditions). Figure 4b shows scan-rate independent CVs collected in MOPS at pH 8.0; these data are shown in Figures S16-S21 for all the conditions relevant to this study. We note that the scan-rate independent CVs of CoGGH do not exhibit the classic S-shape corresponding to voltammograms under pure kinetic conditions,[53-56] for which equation 1 strictly applies. The reason for the absence of a plateau current is that CoGGH exhibits other redox events at potentials more negative than −1.6 V (Figure S22).

In the absence of a plateau current, the determination of I_k from the CVs of CoGGH is somewhat arbitrary; we use the current at a potential of −1.50 V because this is a potential within the catalytic wave but anodic enough as to exclude any contribution from more cathodic features (Figure S22). As the I_k value at −1.50 V is likely lower than the maximum catalytic plateau current, our calculated rate constants are underestimations of the actual catalytic rate constants for the CoGGH film.

Application of equation 1 requires that the catalytic rate is linear with respect to the concentration of substrate S (proton donor, i.e., buffer conjugate acid in this study). This requirement is met under these conditions, as shown in the plots of catalytic current vs buffer-acid concentration ([HA]) of Figures S23-S27. Determination of rate constants using equation 1 also requires an independent determination of the catalyst surface concentration (Γ_{cat}). Instead, we will include Γ_{cat} in the value of the rate constant. This approximation assumes that the catalyst surface concentration remains constant for all of the different conditions explored in our study here. When CoGGH is titrated in, the CV response reaches a maximum current at a CoGGH concentration of 20 to 30 μM for each of the buffers used and for unbuffered solutions as well, supporting the hypothesis that the catalyst is adsorbed and that such adsorption is independent of the presence

and nature of buffer. Figures S28-S33 illustrate the voltammograms collected at increasing [CoGGH] for all the buffers included in our study as well as for pH-adjusted solutions containing KCl and no buffer. By keeping [CoGGH] at 50 μM, we expect that the surface area of the working electrode is saturated with catalyst, keeping a constant Γ_{cat}; we can then define $k_{cat} = k\Gamma_{cat}$; so that equation 1 can be rewritten as follows:

$$I_k = 2FAk_{\mathrm{cat}}[S] \tag{2}$$

Equation 2 needs to be expanded to include the multiple proton donors that coexist in aqueous solutions, i.e. hydronium ions, the conjugate acid form of the buffer (referred to as buffer acid HA), and water molecules themselves, leading to equations 3 and 4.

$$I_k = 2FA\sum_i k_{\mathrm{cat}_i}[\mathrm{S}]_i \tag{3}$$

$$I_k = 2FA(k_{\mathrm{cat}_{\mathrm{HA}}}[\mathrm{HA}] + k_{\mathrm{cat}_{\mathrm{H_2O}}} + k_{\mathrm{cat}_{\mathrm{H_3O^+}}}[\mathrm{H_3O^+}]) \tag{4}$$

In equation 4, the last term is ~ 0 within the experimental pH range of 8 to 10. We will also define, for simplicity, $k_{\mathrm{H_2O}} = k_{\mathrm{cat}_{\mathrm{H_2O}}}$, and $k_{\mathrm{HA}} = k_{\mathrm{cat}_{\mathrm{HA}}}$.

$$I_k = 2FA(k_{\mathrm{HA}}[\mathrm{HA}] + k_{\mathrm{H_2O}}) \tag{5}$$

Measuring the catalytic current in the absence of buffer ([HA] = 0) allows us to determine $k_{\mathrm{H_2O}}$ from equation 5. Once the value of k_{H2O} is known, k_{HA} can be determined for data collected in the presence of buffer. Table S3 shows the values determined for both k_{HA} and k_{H2O} for all the conditions explored in our study. Figure 5 (data listed in Table S4) shows that, for any given buffer acid, the value of k_{HA} is independent of pH and that k_{HA} decreases with increasing buffer-acid pK_a.

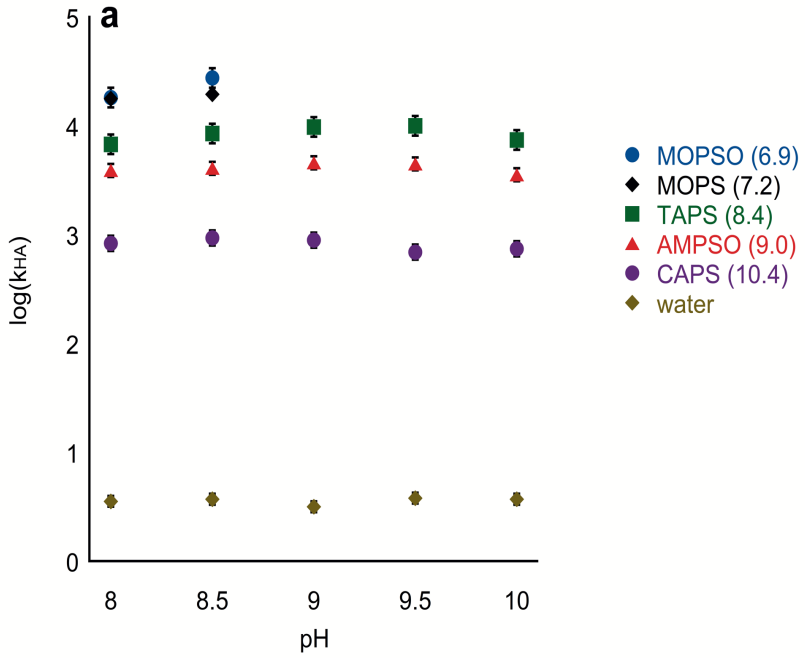

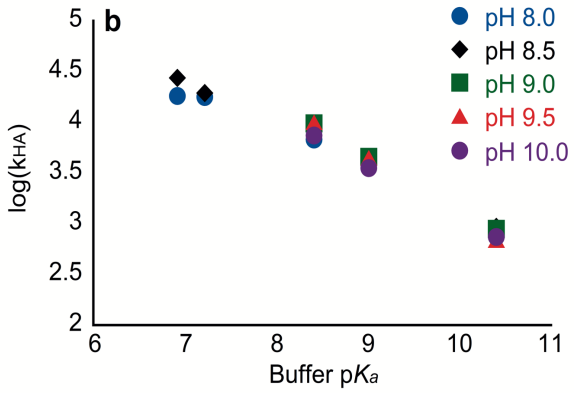

Figure 5. (**a**) Plot of log(k_{HA}) vs pH. Each color corresponds to one buffer. Error bars show the range of the values for each buffer at all pHs. (**b**) Plot of log(k_{HA}) vs buffer-acid pK_a, each color corresponds to a different pH. Error bars are omitted from Figure 5b for clarity.

The linear correlation between k_{HA} and buffer-acid pK_a supports the hypothesis that the acid strength of the proton donor determines the rate of the rate-determining proton-transfer step (RDS) of the catalytic cycle.[14,22] This relationship follows the empirical Brønsted law of general-acid catalysis, further supporting that the buffer-acid species is the proton donor in the RDS of the catalytic cycle. Equation 6 shows the Brønsted law, where α is the slope and C the intercept, the latter with no physical meaning.[22,57]

$$\log(k_{\mathrm{HA}}) = -\alpha(\mathrm{p}K_{\mathrm{a}}) + C \qquad (6)$$

The value of α ranges from 0 to 1 and denotes the extent of rate acceleration attainable for a given increase in driving force by decreasing the proton-donor pK_a.[14,22] Importantly, the coefficient α reveals the extent of protonation of the catalyst in the transition state of the rate-determining step of the catalytic cycle. For values of α between 0.2 and 0.8, a concerted proton-coupled electron transfer (PCET) is possible.[58,59] The average value of α that we find for the Brønsted plots in Figure 5 is 0.48 ± 0.09 (Table S5 shows the data and results of fitting), consistent with a concerted PCET as the rate-determining step of the catalytic cycle, even though a stepwise pathway cannot be ruled out.

We can propose a general mechanism for the electrochemical HER catalyzed by CoGGH as shown in Scheme 1. Even though we cannot determine which step is the RDS, we can say that it is a concerted PCET with the buffer acid acting as proton donor. The values of k_{HA} span over two orders of magnitude from MOPSO (pK_a 6.9) to CAPS (pK_a 10.4), further supporting the hypothesis that the acid strength of the proton donor impacts the rate of proton transfer to the catalyst in the RDS. Also, the values of k_{HA} are at 100 to 10,000 times higher than k_{H2O} in unbuffered solutions, consistent with buffer acid outcompeting water as proton donor in a general-acid catalysis mechanism.

Scheme 1. Proposed Mechanisms for HER catalyzed by CoGGH.[a]

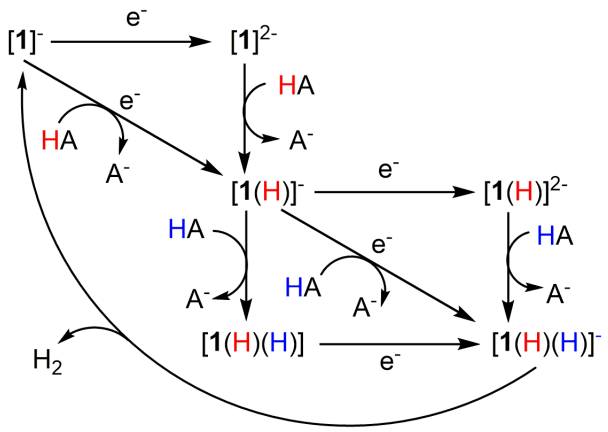

[a]Horizontal and vertical lines correspond to electron- or proton-transfer steps, respectively. [**1**] indicates Co(III)GGH. Diagonal lines correspond to concerted PCET events. Results support there being a concerted PCET involving a buffer acid when present as the RDS; or water acting as proton donor in the absence of buffer. H_2 release may or may not occur as an elementary step. Evolution of H_2 from [**1**(H)(H)] is omitted for simplicity.

Water is the ideal solvent for hydrogen-evolving catalysts and devices but also is a complex medium harboring multiple proton donors and acid-base equilibria. In that context, this measurement of the rate of HER catalysis by CoGGH utilizing buffer acid or water as proton sources is of significant value. These results also quantify the rate acceleration obtained by including a buffer acid for HER catalysis and the dependence of this enhancement on pK_a, highlighting crucial roles that buffers play in proton-transfer reactions in water. These results offer a path to enhancing catalyst performance while highlighting the variation of buffers as a tool for mechanistic study of proton-requiring reactions in water.

EXPERIMENTAL METHODS

Synthesis and Characterization of CoGGH. CoGGH was synthesized, purified, and characterized as described elsewhere.[33]

Cyclic Voltammetry. CV experiments were conducted using a three-electrode setup with a $Ag/AgCl/KCl_{(1M)}$ reference electrode (CH instruments), a Pt wire counter electrode (surface area ~0.32 cm^2), and a mercury drop electrode (BASi CGME MF-9058 used in static mode) as the working electrode (surface area 2.45×10^{-2} cm^2). A CH Instruments 620 D potentiostat was used for all electrochemical experiments. The CV working solution was purged with N_2 for ~15 min before each experiment, and the cell was kept under a N_2 atmosphere during experiments. All voltammograms were collected scanning from 0 V to negative potentials and then back to 0 V.

Controlled Potential Electrolysis. Controlled potential electrolysis experiments were performed in a two-compartment cell with a three-electrode system: a $Ag/AgCl/KCl_{(1M)}$ reference electrode, a glassy carbon rod counter electrode (surface area ~1.9 cm^2), and a mercury pool working electrode with a surface area of approximately 1.0 cm^2 connected to the circuit by an insulated

platinum wire. The volume of the solution in each compartment was 5 mL, purged with an 80:20% N_2/CH_4 mixture (from Airgas) before each experiment with the CH_4 serving as an internal standard. The amount of generated H_2 was determined by GC using a calibration curve obtained by injecting known volumes of H_2 at 1 atm. The GC instrument is a Shimadzu GC-2014 with a Thermal Conductivity Detector and a Restek RT-Msieve 5 Å column.

The Dip-and-Stir (D-S) Test. This test is a version of the typical rinse test, adapted to a mercury drop electrode. After collecting a CV or just exposing the Hg drop to the catalyst-containing solution, the electrochemical cell is removed, and the counter and reference electrodes are carefully wiped while the Hg drop remains at the tip of the capillary. The electrodes are then dipped into a new electrochemical cell containing fresh solution with no catalyst. The solution is stirred for three minutes, using a magnetic stir bar, to remove any catalyst-containing droplets from the electrodes. A CV is then collected, and any above-background activity detected is due to catalyst adsorbed to the Hg drop. The validity of the method was tested by performing this procedure with methyl viologen in solution, in which case no residual activity was found after the D-S test (Figure S8).

ASSOCIATED CONTENT

Supporting Information

The Supporting Information is available free of charge at https://pubs.acs.org...

Tables S1 – S5, Figures S1 – S33, information on buffers and titration data, additional electrochemical data, tables of rate constants, results from data fitting.

AUTHOR INFORMATION

Corresponding Author

Kara L. Bren – Department of Chemistry, University of Rochester, Rochester, New York 14627-0216, United States; ORCID iD: https://orcid.org/0000-0002-8082-3634; **Email:** bren@chem.rochester.edu

Authors

Jose L. Alvarez-Hernandez – Department of Chemistry, University of Rochester, Rochester, New York 14627-0216, United States; ORCID iD: https://orcid.org/0000-0002-1761-9024.

Ji Won Han – Department of Chemistry, University of Rochester, Rochester, New York 14627-0216, United States; ORCID iD: https://orcid.org/0000-0003-1445-601X.

Andrew E. Sopchak – Department of Chemistry, University of Rochester, Rochester, New York 14627-0216, United States

Yixing Guo – Department of Chemistry, University of Rochester, Rochester, New York 14627-0216, United States

Notes

The authors declare no competing financial interest.

ACKNOWLEDGEMENTS

This work is supported by the U.S. National Science Foundation grant CHE-1708256. The authors thank Emily Edwards, Jesse Stroka, Jennifer Le, and Banu Kandemir for helpful discussions.

REFERENCES

1. Le, J. M.; Bren, K. L. Engineered Enzymes and Bioinspired Catalysts for Energy Conversion. *ACS Energy Lett.*, **2019**, 4, 2168-2180.
2. Tong, L.; Duan, L.; Zhou, A.; Thummel, R. P. First-row transition metal polypyridine complexes that catalyze proton to hydrogen reduction. *Coord. Chem. Rev.*, **2020**, 402, 213079.
3. Zhai, W.; Lai, W.; Cao, R. Energy-Related Small Molecule Activation Reactions: Oxygen Reduction and Hydrogen and Oxygen Evolution Reactions Catalyzed by Porphyrin- and Corrole-Based Systems. *Chem. Rev.*, **2017**, 117, 3717-3797.
4. Weinberg, D. R.; Gagliardi, C. J.; Hull, J. F.; Murphy, C. F.; Kent, C. A.; Westlake, B. C.; Paul, A.; Ess, D. H.; McCafferty, D. C.; Meyer, T. J. Proton-Coupled Electron Transfer. *Chem. Rev.*, **2012**, 112, 4016-4093.
5. Mayer, J. M. Proton-Coupled Electron Transfer: A Reaction Chemist's View. *Annu. Rev. Phys. Chem.*, **2004**, 55, 363-390.
6. Costentin, C.; Robert, M.; Savéant, J.-M. Update 1 of: Electrochemical Approach to the Mechanistic Study of Proton-Coupled Electron Transfer. *Chem. Rev.*, **2010**, 110, PR1-PR40.
7. Stubbert, B. D.; Peters, J. C.; Gray, H. B. Rapid Water Reduction to H2 Catalyzed by a Cobalt Bis(iminopyridine) Complex. *J. Am. Chem. Soc.*, **2011**, 133, 18070-18073.
8. Schnidrig, S.; Bachmann, C.; Müller, P.; Weder, N.; Spingler, B.; Joliat-Wick, E.; Mosberger, M.; Windisch, J.; Alberto, R.; Probst, B. Structure–Activity and Stability Relationships for Cobalt Polypyridyl-Based Hydrogen-Evolving Catalysts in Water. *ChemSusChem*, **2017**, 10, 4570-4580.
9. Horvath, S.; Fernandez, L. E.; Appel, A.; Hammes-Schiffer, S. pH-Dependent Reduction Potentials and Proton-Coupled Electron Transfer Mechanisms in Hydrogen-Producing Nickel Molecular Electrocatalysts. *Inorg. Chem.*, **2013**, 52, 3643-3652.
10. Tsay, C.; Yang, J. Y. Electrocatalytic Hydrogen Evolution under Acidic Aqueous Conditions and Mechanistic Studies of a Highly Stable Molecular Catalyst. *J. Am. Chem. Soc.*, **2016**, 138, 14174-14177.
11. Tsay, C.; Ceballos, B. M.; Yang, J. Y. pH-Dependent Reactivity of a Water-Soluble Nickel Complex: Hydrogen Evolution vs Selective Electrochemical Hydride Generation. *Organometallics*, **2018**, 38, 1286-1291.
12. Rountree, E. S.; Martin, D. J.; McCarthy, B. D.; Dempsey, J. L. Linear Free Energy Relationships in the Hydrogen Evolution Reaction: Kinetic Analysis of a Cobaloxime Catalyst. *ACS Catal.*, **2016**, 6, 3326-3335.
13. Alvarez-Hernandez, J. L.; Sopchak, A. E.; Bren, K. L. Buffer pK_a Impacts the Mechanism of Hydrogen Evolution Catalyzed by a Cobalt Porphyrin-Peptide. *Inorg. Chem.*, **2020**, 59, 8061-8069.
14. Medina-Ramos, J.; Oyesanya, O.; Alvarez, J. C. Buffer Effects in the Kinetics of Concerted Proton-Coupled Electron Transfer: The Electrochemical Oxidation of Glutathione Mediated by $[IrCl_6]^{2-}$ at Variable Buffer pK_a and Concentration. *J. Phys. Chem. C*, **2013**, 117, 902-912.

15. Le, J. M.; Alachouzos, G.; Chino, M.; Frontier, A. J.; Lombardi, A.; Bren, K. L. Tuning Mechanism through Buffer Acid Dependence of Hydrogen Evolution by a Cobalt Mini-enzyme. *Biochemistry*, **2020**, 59, 1289-1297.
16. Jackson, M. N.; Jung, O.; Lamotte, H. C.; Surendranath, Y. Donor-Dependent Promotion of Interfacial Proton-Coupled Electron Transfer in Aqueous Electrocatalysis. *ACS Catal.*, **2019**, 9, 3737-3743.
17. Jackson, M. N.; Surendranath, Y. Donor-Dependent Kinetics of Interfacial Proton-Coupled Electron Transfer. *J. Am. Chem. Soc.*, **2016**, 138, 3228-3234.
18. Costentin, C.; Dridi, H.; Savéant, J.-M. Molecular Catalysis of H2 Evolution: Diagnosing Heterolytic versus Homolytic Pathways. *J. Am. Chem. Soc.*, **2014**, 136, 13727-13734.
19. Costentin, C.; Savéant, J.-M. Homogeneous Molecular Catalysis of Electrochemical Reactions: Manipulating Intrinsic and Operational Factors for Catalyst Improvement. *J. Am. Chem. Soc.*, **2018**, 140, 16669-16675.
20. Queyriaux, N.; Sun, D.; Fize, J.; Pécaut, J.; Field, M. J.; Chavarot-Kerlidou, M.; Artero, V Electrocatalytic Hydrogen Evolution with a Cobalt Complex Bearing Pendant Proton Relays: Acid Strength and Applied Potential Govern Mechanism and Stability. *J. Am. Chem. Soc.*, **2020**, 142, 274-282.
21. Kilgore, U. J.; Roberts, J. A. S.; Pool, D. H.; Appel, A. M.; Stewart, M. P.; DuBois, M. R.; Dougherty, W. G.; Kassel, W. S.; Bullock, R. M.; DuBois, D. L. $[Ni(P^{Ph2}N^{C6H4X2})_2]^{2+}$ Complexes as Electrocatalysts for H_2 Production: Effect of Substituents, Acids, and Water on Catalytic Rates. *J. Am. Chem. Soc.*, **2011**, 133, 5861-5872.
22. Martin, D. J.; Wise, C. F.; Pegis, M. L.; Mayer, J. M. Developing Scaling Relationships for Molecular Electrocatalysis through Studies of Fe-Porphyrin-Catalyzed O_2 Reduction. *Acc. Chem. Res.*, **2020**, 53, 1056-1065.
23. Tsay, C.; Livesay, B. N.; Ruelas, S.; Yang, J. Y. Solvation Effects on Metal Hydricity. *J. Am. Chem. Soc.*, **2015**, 137, 14114-14121.
24. Burgess, S. A.; Appel, A. M.; Linehan, J. C.; Wiedner, E. S. Changing the Mechanism for CO2 Hydrogenation Using Solvent-Dependent Thermodynamics. *Angew. Chem. Int. Ed.*, **2017**, 56, 15002-15005.
25. King, A. E.; Surendranath, Y.; Piro, N. A.; Bigi, J. P.; Long, J. R; Chang, C. J. A mechanistic study of proton reduction catalyzed by a pentapyridine cobalt complex: evidence for involvement of an anation-based pathway. *Chem. Sci.*, **2013**, 4, 1578-1587.
26. Lee, C. H.; Dogutan, D. K.; Nocera, D. G. Hydrogen Generation by Hangman Metalloporphyrins. *J. Am. Chem. Soc.*, **2011**, 133, 8775-8777.
27. Roubelakis, M. M.; Bediako, D. K.; Dogutan, D. K.; Nocera, D. G. Proton-coupled electron transfer kinetics for the hydrogen evolution reaction of hangman porphyrins. *Energy Environ. Sci.*, **2012**, 5, 7737-7740.
28. Yang, J. Y.; Smith, S. E.; Liu, T.; Dougherty, W. G.; Hoffert, W. A.; Kassel, W. S.; DuBois, M. R.; DuBois, D. L.; Bullock, R. M. Two Pathways for Electrocatalytic Oxidation of Hydrogen by a Nickel Bis(diphosphine) Complex with Pendant Amines in the Second Coordination Sphere. *J. Am. Chem. Soc.*, **2013**, 135, 9700-9712.
29. Jacques, P-A.; Artero, V.; Pécaut, J.; Fontecave, M. Cobalt and nickel diimine-dioxime complexes as molecular electrocatalysts for hydrogen evolution with low overvoltages. *Proc. Natl. Acad. Sci. U.S.A.*, **2009**, 106, 20627-20632.

30. Dolui, D.; Ghorai, S.; Dutta, A. Tuning the reactivity of cobalt-based H_2 production electrocatalysts via the incorporation of the peripheral basic functionalities. *Coord. Chem. Rev.*, **2020**, 416, 1-20.
31. Ginovska-Pangovska, B.; Dutta, A.; Reback, M. L.; Linehan, J. C.; Shaw, W. J. Beyond the Active Site: The Impact of the Outer Coordination Sphere on Electrocatalysts for Hydrogen Production and Oxidation. *Acc. Chem. Res.*, **2014**, 47, 2621-2630.
32. Hammes-Schiffer, S. Proton-Coupled Electron Transfer: Moving Together and Charging Forward. *J. Am. Chem. Soc.*, **2015**, 137, 8860-8871.
33. Kandemir, B.; Kubie, L.; Guo, Y.; Sheldon, B.; Bren, K. L. Hydrogen Evolution from Water under Aerobic Conditions Catalyzed by a Cobalt ATCUN Metallopeptide. *Inorg. Chem.*, **2016**, 55, 1355-1357.
34. Kleingardner, J. G.; Kandemir, B.; Bren, K. L. Hydrogen Evolution from Neutral Water under Aerobic Conditions Catalyzed by Cobalt Microperoxidase-11. *J. Am. Chem. Soc.* , **2014**, 136, 4-7.
35. Chakraborty, S.; Edwards, E. H.; Kandemir, B.; Bren, K. L. Photochemical Hydrogen Evolution from Neutral Water with a Cobalt Metallopeptide Catalyst. *Inorg. Chem.*, **2019**, 58, 16402-16410.
36. Karunadasa, H. I.; Chang, C. J.; Long, J. R. A molecular molybdenum-oxo catalyst for generating hydrogen from water. *Nature*, **2010**, 464, 1329-1333.
37. Clary, K. E.; Karayilan, M.; McCleary-Petersen, K.; Petersen, H. A.; Glass, R. S.; Pyun, J.; Lichtenberger, D. L. Increasing the rate of the hydrogen evolution reaction in neutral water with protic buffer electrolytes. *Proc. Natl. Acad. Sci. U.S.A.*, **2020**,
38. McCrory, C. C. L.; Uyeda, C.; Peters, J. C. Electrocatalytic Hydrogen Evolution in Acidic Water with Molecular Cobalt Tetraazamacrocycles. *J. Am. Chem. Soc.*, **2012**, 134, 3164-3170.
39. Schneider, C. R.; Lewis, L. C.; Shafaat, H. S. The good, the neutral, and the positive: buffer identity impacts CO_2 reduction activity by nickel(II) cyclam. *Dalton Trans.*, **2019**,
40. Costentin, C.; Robert, M.; Savéant, J.-M.; Tatin, A. Efficient and selective molecular catalyst for the CO_2-to-CO electrochemical conversion in water. *Proc. Natl. Acad. Sci. U.S.A.*, **2015**, 112, 6882-6886.
41. Wang, D.; Groves, J. T. Efficient water oxidation catalyzed by homogeneous cationic cobalt porphyrins with critical roles for the buffer base. *Proc. Natl. Acad. Sci. U.S.A.*, **2013**, 110, 11579-15584.
42. Song, N.; Concepcion, J. J.; Binstead, R. A.; Rudd, J. A.; Vanucci, A. K.; Dares, C. J.; Coggins, M. K.; Meyer, T. J. Base-enhanced catalytic water oxidation by a carboxylate–bipyridine Ru(II) complex. *Proc. Natl. Acad. Sci. U.S.A.*, **2015**, 117, 4935-4940.
43. Zhang, L.-H.; Yu, F.; Shi, Y.; Li, F.; Li, H. Base-enhanced electrochemical water oxidation by a nickel complex in neutral aqueous solution. *Chem. Commun.*, **2019**, 55, 6122-6125.
44. Chen, Z.; Concepcion, J. J.; Hu, X.; Yang, W.; Hoertz, P. G.; Meyer, T. J. Concerted O atom–proton transfer in the O—O bond forming step in water oxidation. *Proc. Natl. Acad. Sci. U.S.A.*, **2010**, 107, 7225-7229.
45. Baffert, C.; Artero, V.; Fontecave, M. Cobaloximes as Functional Models for Hydrogenases. 2. Proton Electroreduction Catalyzed by Difluoroborylbis(dimethylglioximato)cobalt(II) Complexes in Organic Media. *Inorg. Chem.*, **2007**, 46, 1817-1824.

46. Wu, Y.; Hu, G.; Rooney, C. L.; Brudvig, G. W.; Wang, H. Heterogeneous Nature of Electrocatalytic CO/CO_2 Reduction by Cobalt Phthalocyanines. *ChemSusChem*, **2020**, 13,
47. Berben, L. A.; Peters, J. C. Hydrogen evolution by cobalt tetraimine catalysts adsorbed on electrode surfaces. *Chem. Commun.*, **2009**, 46, 398-400.
48. Kaeffer, N.; Morozan, A.; Fize, J.; Martinez, J.; Guetaz, L.; Artero, V. The Dark Side of Molecular Catalysis: Diimine−Dioxime Cobalt Complexes Are Not the Actual Hydrogen Evolution Electrocatalyst in Acidic Aqueous Solutions. *ACS Catal.*, **2016**, 6, 3727-3737.
49. Lee, K. J.; McCarthy, B. D.; Dempsey, J. L. On decomposition, degradation, and voltammetric deviation: the electrochemist's field guide to identifying precatalyst transformation. *Chem. Soc. Rev.*, **2019**, 48, 2927-2945.
50. Anxolabéhere-Mallart, E.; Costentin, C.; Fournier, M.; Robert, M. Cobalt-Bisglyoximato Diphenyl Complex as a Precatalyst for Electrocatalytic H_2 Evolution. *J. Phys. Chem. C*, **2014**, 118, 13377-13381.
51. Martin, D. J.; McCarthy, B. D.; Donley, C. L; Dempsey, J. L. Electrochemical hydrogenation of a homogeneous nickel complex to form a surface adsorbed hydrogen-evolving species. *Chem. Comm.*, **2015**, 51, 5290-5293.
52. Artero, V.; Fontecave, M. Solar fuels generation and molecular systems: is it homogeneous or heterogeneous catalysis? *Chem. Soc. Rev.*, **2013**, 42, 2338-2356.
53. Costentin, C.; Savéant, J.-M. Cyclic Voltammetry Analysis of Electrocatalytic Films. *J. Phys. Chem. C*, **2015**, 119, 12174-12182.
54. Costentin, C.; Savéant, J. M. Cyclic Voltammetry of Electrocatalytic Films: Fast Catalysis Regimes. *ChemElectroChem*, **2015**, 2, 1774-1784.
55. Savéant, J.-M. Molecular Catalysis of Electrochemical Reactions. Mechanistic Aspects. *Chem. Rev.*, **2008**, 108, 2348-2378.
56. Costentin, C.; Savéant, J.-M. Multielectron, Multistep Molecular Catalysis of Electrochemical Reactions: Benchmarking of Homogeneous Catalysts. *ChemElectroChem*, **2014**, 1, 1226-1236.
57. Maskill, H. *The Investigation of Organic Reactions and their Mechanisms*. 2006, Oxford, U.K.: Blackwell Publishing Ltd. 370.
58. Jencks, W. P. Requirements for General Acid-Base Catalysis of Complex Reactions. *J. Am. Chem. Soc.*, **1972**, 94, 4731-4732.
59. Jencks, W. P. General Acid-Base Catalysis of Complex Reactions in Water. *Chem. Rev.*, **1972**, 72, 705-718.